

# Manipulating Solid Forms of Contact Insecticides for Infectious Disease Prevention

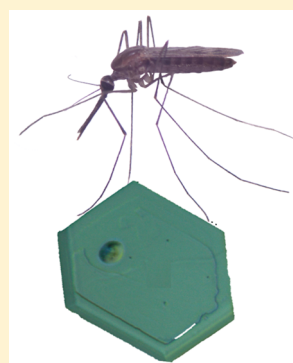
Xiaolong Zhu,<sup>†</sup> Chunhua T. Hu,<sup>†</sup> Jingxiang Yang,<sup>†</sup> Leo A. Joyce,<sup>‡</sup> Mengdi Qiu,<sup>†</sup> Michael D. Ward,<sup>\*,†</sup> and Bart Kahr<sup>\*,†</sup>

<sup>†</sup>Department of Chemistry and Molecular Design Institute, New York University, 100 Washington Square East, New York, New York 10003 United States

<sup>‡</sup>Department of Process Research & Development, Merck & Co, Inc., Rahway, New Jersey 07065, United States

## S Supporting Information

**ABSTRACT:** Malaria control is under threat by the development of vector resistance to pyrethroids in long-lasting insecticidal nets, which has prompted calls for a return to the notorious crystalline contact insecticide DDT. A faster acting difluoro congener, DFDT, was developed in Germany during World War II, but in 1945 Allied inspectors dismissed its superior performance and reduced toxicity to mammals. It vanished from public health considerations. Herein, we report the discovery of amorphous and crystalline forms of DFDT and a mono-fluorinated chiral congener, MFDT. These solid forms were evaluated against *Drosophila* as well as *Anopheles* and *Aedes* mosquitoes, the former identified as disease vectors for malaria and the latter for Zika, yellow fever, dengue, and chikungunya. Contact insecticides are transmitted to the insect when its feet contact the solid surface of the insecticide, resulting in absorption of the active agent. Crystalline DFDT and MFDT were much faster killers than DDT, and their amorphous forms were even faster. The speed of action (a.k.a. knockdown time), which is critical to mitigating vector resistance, depends inversely on the thermodynamic stability of the solid form. Furthermore, one enantiomer of the chiral MFDT exhibits faster knockdown speeds than the other, demonstrating chiral discrimination during the uptake of the insecticide or when binding at the sodium channel, the presumed destination of the neurotoxin. These observations demonstrate an unambiguous link between thermodynamic stability and knockdown time for important disease vectors, suggesting that manipulation of the solid-state chemistry of contact insecticides, demonstrated here for DFDT and MFDT, is a viable strategy for mitigating insect-borne diseases, with an accompanying benefit of reducing environmental impact.



## INTRODUCTION

Agents for combatting infectious diseases may be in full view, but not always seen. Artemisinin-based malaria therapies were not so much discovered as rediscovered, inspired by ancient pharmacopeias.<sup>1</sup> Malaria and other vector-borne diseases also can be mitigated by insecticides. During the 20th century DDT (1,1,1-trichloro-2,2-bis(4-chlorophenyl)ethane; **Figure 1a**), which was patented by the Swiss company J. R. Geigy S. A. in 1939, was the most commonly used contact insecticide.<sup>2,3</sup> A contact insecticide overlooked by the public health community is DFDT (1,1,1-trichloro-2,2-bis(4-fluorophenyl)ethane; **Figure 1a**), known as Gix among other names.<sup>3</sup> DFDT was developed by the German company, Höchst A. G., to circumvent paying of royalties for the use of DDT. Höchst manufactured 40 tons/month of DFDT during World War II for the German army in North Africa and on the eastern front.<sup>4</sup> Meanwhile, American authorities considered DDT “magic”.<sup>5</sup> Combined military and post-war civilian spraying campaigns covered the planet with *two million tons* of DDT.<sup>6</sup>

DFDT manufacture ended abruptly in the post-war chaos and was never revived. Victorious Allied military officials dismissed German claims of DFDT’s fast action against pests and lower toxicity to mammals.<sup>7</sup> Müller, in his 1948 Nobel

address acknowledging his discovery of DDT,<sup>8</sup> argued that faster-acting DFDT should be the insecticide of the future. Forward-thinking scientists recognized that speed of insect knockdown is essential for combatting resistance to exogenous chemical agents.<sup>9,10</sup> Inexpensive DDT, however, was achieving everything asked of it and was marshalled for the eradication of malaria by the World Health Organization (WHO) in 1955.<sup>11</sup> DDT nevertheless faltered in the face of insect resistance<sup>12</sup> and experienced a backlash in the wake of serious environmental concerns, foretold by Rachel Carson in *Silent Spring*.<sup>13</sup> From 2006 to 2015, indoor residual spraying (IRS) of DDT was recommended by the WHO as a primary tool for controlling malaria.<sup>14,15</sup> In a 2019 report, however, the WHO retreated from their earlier position, recommending DDT for IRS only when other compounds were ineffective.<sup>16</sup> Nonetheless, an accurate reading of history suggests that DDT would have remained effective for infectious disease mitigation if it had not been used in such a cavalier manner for agricultural applications.

Received: July 29, 2019

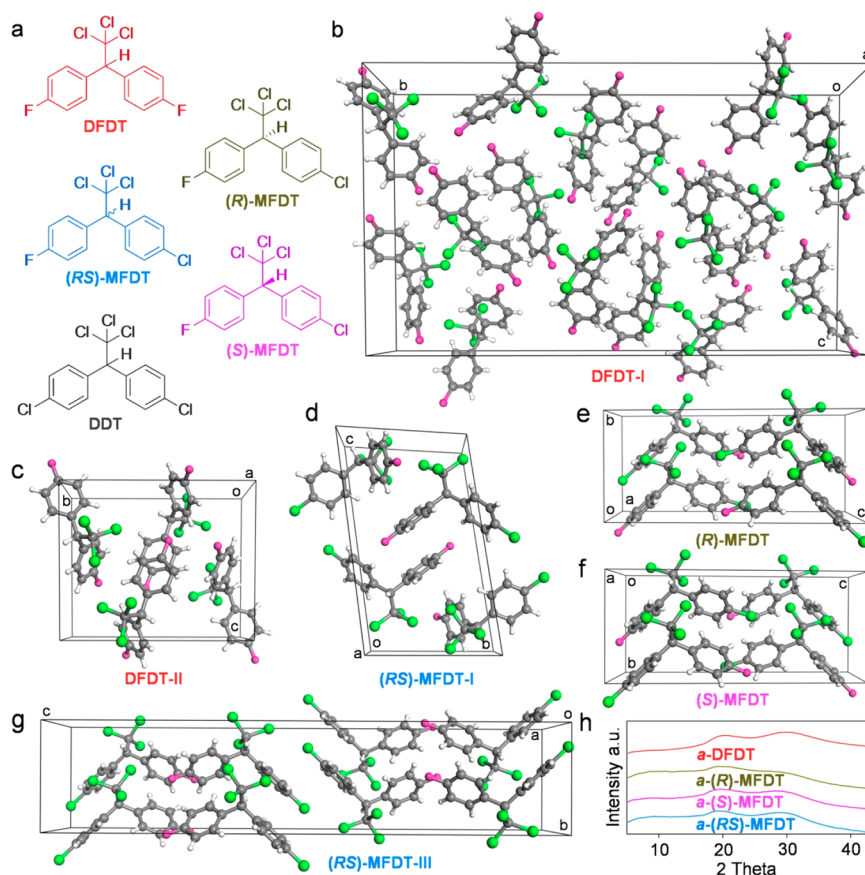


**Figure 1.** Solid-state forms of DFDT and MFDT. (a) Molecular structures. (b) DFDT-I (space group,  $P2_1/c$ ) is isostructural with (RS)-MFDT-II (Supporting Information, Figure S7). (c) DFDT-II ( $P2_1/c$ ). (d) (RS)-MFDT-I ( $P1$ ). (e) (R)-, and (f) (S)-MFDT ( $P2_1$ ). (g) (RS)-MFDT-III ( $Pbca$ ). (h) Broad powder X-ray diffraction (PXRD) halos observed for amorphous forms. Atom colors: hydrogen, white; carbon, gray; fluorine, red; chlorine, green.

Numerous strategies have been pursued for the treatment of malaria infection, largely through the design of therapeutics aimed at the cellular level of the parasite.<sup>17–20</sup> The role of crystals and their properties in the control of malaria have been invoked, however, during investigations aimed at antimalarial drugs that can prevent the crystallization of hemozoin, which forms in the food vacuole of the *Plasmodium falciparum* parasite from free heme generated when the parasite degrades hemoglobin. In this manner, the crystallization of the very insoluble hemozoin effectively removes the parent heme, which otherwise would be toxic to the parasite.<sup>21–25</sup>

An alternative approach using solid-state chemistry is considered here. DDT and DFDT are contact insecticides that kill when insects directly contact the solid, but this interaction had not been articulated in the context of solid-state chemistry until the serendipitous discovery in our laboratory of a second crystalline form of DDT (hence designated as Form II) that killed *Drosophila* (the fruit fly) more quickly than the only form (now Form I) previously identified.<sup>26</sup> This suggested a pathway to faster-acting agents based on engineering of solid-state forms that could slow resistance development because of their faster action. Moreover, improved efficacy means that smaller quantities are required to achieve the same effect, promising a reduction in environmental impact. New insecticides are urgently needed as mosquitoes worldwide are becoming resistant to pyrethroids embedded in long lasting insecticidal nets (LLINs), threatening gains against malaria.<sup>27</sup> Herein we demonstrate that

newly discovered solid-state forms of DFDT and its chiral mono-fluoro analog MFDT<sup>28</sup> (1,1,1-trichloro-2,2-(4-chlorophenyl)-(4-fluorophenyl)-ethane; Figure 1a) act much more rapidly than DDT against *Drosophila* as well as *Anopheles quadrimaculatus*, a vector for malaria, and *Aedes aegypti*, a vector for Zika virus, yellow fever, dengue, and chikungunya.<sup>29</sup> These results also demonstrate an unambiguous link between thermodynamic stability and knockdown speed for important disease vectors, suggesting that manipulation of the solid-state chemistry of contact insecticides is a viable strategy for mitigating insect-borne diseases, with an accompanying benefit of reducing environmental impact.

## RESULTS AND DISCUSSION

DFDT and MFDT were synthesized from trichloroacetate and *p*-fluorobenzaldehyde to give 1-(4-fluorophenyl)-2,2,2-trichloroethanol.<sup>30</sup> Subsequent reaction with fluorobenzene or chlorobenzene afforded DFDT and MFDT, respectively.<sup>31</sup> Two polymorphic crystalline forms of DFDT (DFDT-I, -II) and three polymorphic forms of racemic MFDT ((RS)-MFDT-I, -II, and -III) were discovered (see Experimental Section and Supporting Information, Figures S1–S4). DFDT-I single crystals could be obtained from a variety of solvents and DFDT-II single crystals from diethyl ether. (RS)-MFDT-I could be crystallized from a variety of solvents. The (R)- and (S)-MFDT enantiomers were resolved by chromatography on a chiral stationary phase (Supporting Information, Figure S6), and single crystals were grown from a variety of solvents.

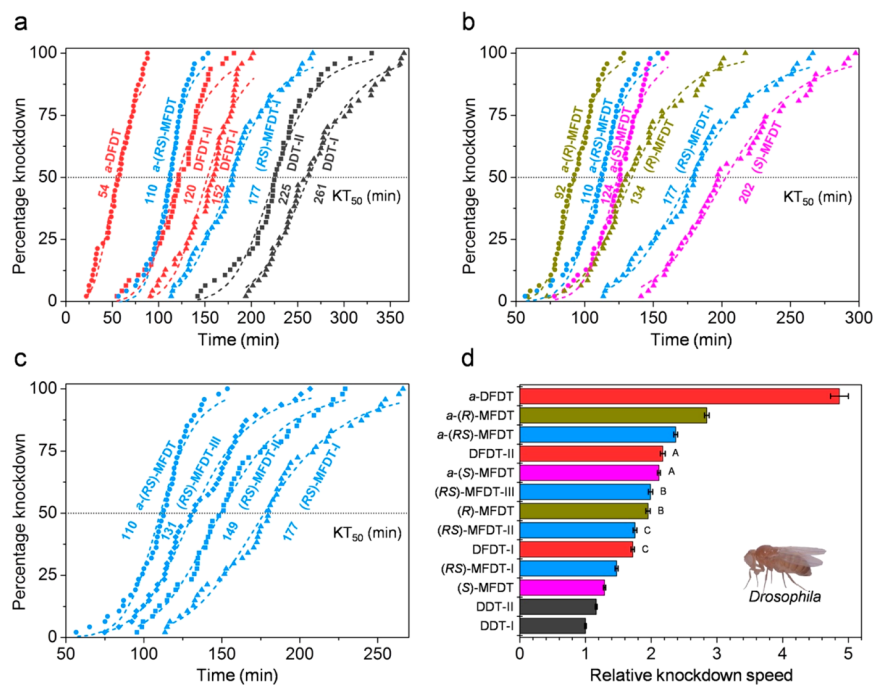


**Figure 2.** Lethalities of solid-state forms of DFDT, MFDT, and DDT for *Drosophila melanogaster*. (a–c) Each symbol corresponds to one female. Dashed lines indicate logistic regression of knockdown-time curves. The median knockdown time for each curve is denoted by its intersection with the horizontal  $KT_{50}$  marker. (d) Comparison of the knockdown speeds ( $1/KT_{50}$ ) relative to DDT I. Error bars represent 95% confidence intervals (CI). Values with the same letter have overlapping 95% CIs, and differences are considered insignificant. Inset: Photo of a typical female fly.

Curiously, single crystals of (RS)-MFDT-II and -III were obtained by crystallization from the melt at  $>30$  and  $25$  °C, respectively, using seed crystals of either the R or S isomer. These crystalline forms, six total, were characterized by single-crystal X-ray diffraction (Figure 1; Supporting Information, Figure S7). The melting points of DFDT-I and -II were similar ( $T_m = 40$  and  $39$  °C, respectively; Supporting Information, Figure S8) but microcrystalline DFDT-II slowly transformed to DFDT-I at room temperature (Supporting Information, Figures S9–S11), indicating that the latter is more thermodynamically stable. (RS)-MFDT-II and -III microcrystals slowly transformed to (RS)-MFDT-I at room temperature (Supporting Information, Figures S12–S14), although III transformed much more rapidly. The apparent thermodynamic stabilities of crystalline MFDT racemates parallel their melting points,  $T_m$ : RS-I ( $62$  °C)  $>$  RS-II ( $54$  °C)  $>$  RS-III ( $35$  °C) (Supporting Information, Figure S8). Collectively, this is strong evidence (RS)-MFDT-III is less stable than its Form II at room temperature, especially given the low melting point of Form III. The  $T_m$  of the enantiomorphs was  $47$  °C (Supporting Information, Figure S8). Amorphous DFDT (*a*-DFDT), prepared by supercooling melts or fine mist spraying of solutions (Supporting Information, Table S3), afforded broad X-ray scattering halos (Figure 1h; Supporting Information, Figure S2), and was stable for 25 days at room temperature. Amorphous resolved and racemic MFDT (*a*-(R)- and *a*-(S)-MFDT, and *a*-(RS)-MFDT, respectively; Figure 1h) were stable for 10 days at room temperature. These observations contrast with *a*-DDT, which transformed to crystalline DDT Form I within 5 h at room temperature. Notably, *a*-DFDT is stable for at least 120 days by addition of 10 wt% PEG 100 emulsifier, promising its use as a contact insecticide.

Female *Drosophila melanogaster* were exposed to  $2.0 \pm 0.1$  mg of DFDT, MFDT, and DDT separately, in their crystalline and amorphous forms (Supporting Information, Figure S15). The insects were monitored with a video camera until the entire population ceased to move. The videos then were analyzed to determine the knockdown times—a proxy for lethality—for each individual insect (Videos S1–S5).<sup>32</sup> Like DDT, DFDT and MFDT induced hyperactivity followed by paralysis, and then death.  $KT_{50}$  values, the times required for death of 50% of the insects, are the standard for assessing insecticide lethality (the lifetimes of individual insects differ because of the random nature of their contact with insecticide surfaces and varied susceptibility of a population). Here, the  $KT_{50}$  values were calculated by logistic regression of knockdown-time curves (Supporting Information, Figure S16, Table S4).<sup>33</sup> The  $KT_{50}$  values spanned the range of 261 to 54 min, decreasing in the order DDT-I  $>$  DDT-II  $>$  (S)-MFDT  $>$  (RS)-MFDT-I  $>$  DFDT-I  $\sim$  (RS)-MFDT-II  $>$  (R)-MFDT  $\sim$  (RS)-MFDT-III  $>$  *a*-(S)-MFDT  $\sim$  DFDT-II  $>$  *a*-(RS)-MFDT  $>$  *a*-(R)-MFDT  $>$  *a*-DFDT (Figure 2a–c; Supporting Information, Figure S17). Knockdown speeds, reciprocals of  $KT_{50}$  values,<sup>34</sup> decreased in inverse order (Figure 2d). The amorphous forms are always faster than their respective crystalline counterparts, with *a*-DFDT the fastest. The MFDT R forms, whether crystalline or amorphous, have higher knockdown speeds than their respective S forms suggesting enantioselectivity in uptake by the insect or neurotoxicity. Overall, the lethalities of the different solid forms of a given compound, as deduced from their knockdown speeds, were inversely correlated with their thermodynamic stability.<sup>26,35</sup>

Female *Anopheles* and *Aedes* mosquitoes exposed to  $1.0 \pm 0.1$  mg of various crystalline forms followed the same knockdown trend as *Drosophila*, with  $KT_{50}$  values decreasing in the order DDT-I  $>$  (RS)-MFDT-I  $>$  DFDT-I  $>$  DFDT-II

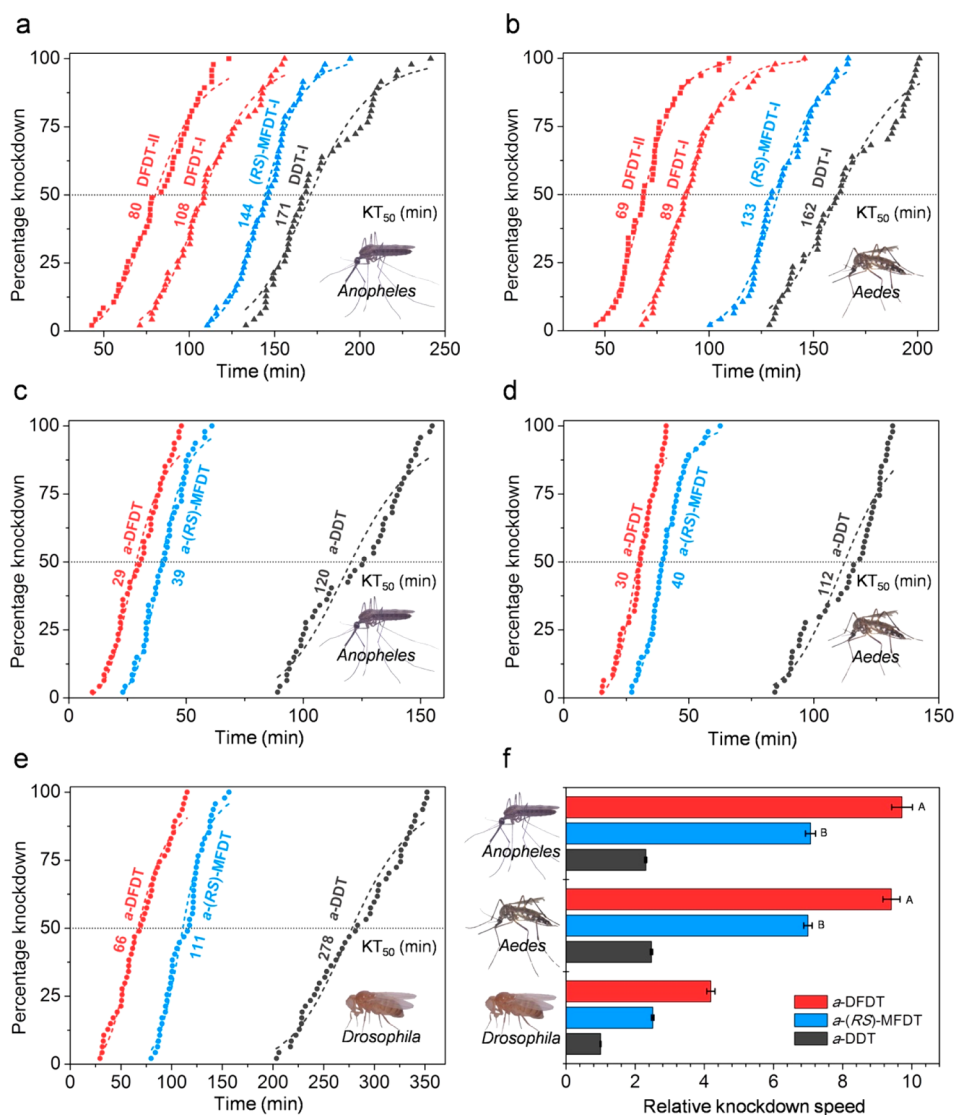


**Figure 3.** (a, b) Lethalities of crystalline forms of DFDT, (RS)-MFDT, and DDT for *Anopheles quadrimaculatus* (a) and *Aedes aegypti* (b). (c–e) Lethalities of amorphous forms *a*-DFDT, *a*-(RS)-MFDT, and *a*-DDT for *Anopheles quadrimaculatus* (c), *Aedes aegypti* (d), and *Drosophila melanogaster* (e). Each symbol corresponds to one female. Dashed lines indicate logistic regression of knockdown-time curves. The median knockdown time for each curve is denoted by its intersection with the horizontal KT<sub>50</sub> marker. (f) Relative knockdown speeds of amorphs. Error bars represent 95% confidence intervals (CI). Values with the same letter have overlapping 95% CIs, and differences are considered insignificant. Insets: Photos of typical females.

(Figure 3a,b; Videos S6 and S7). Given that DFDT and MFDT amorphs were more active than their crystalline forms against *Drosophila*, the lethalities of the amorphous forms were evaluated as well for *Anopheles* and *Aedes* mosquitoes. Female mosquitoes were introduced into Petri dishes coated with  $1.0 \pm 0.1$  mg of the amorphous forms, and their motions recorded (Videos S8–S10). KT<sub>50</sub> values for *a*-DFDT and *a*-(RS)-MFDT against *Anopheles* were 29 and 39 min, and against *Aedes* they were 30 and 40 min, respectively (Figure 3 c,d; Supporting Information, Figure S20). Corresponding KT<sub>50</sub> values for *a*-DDT were much larger (120 and 112 min). Accordingly, the knockdown speeds for *a*-DFDT and *a*-(RS)-MFDT are 4 and 3 times faster than for *a*-DDT, respectively (Figure 3f).

## CONCLUSIONS

In a warming world, the range of *Anopheles* mosquitoes may increase.<sup>36</sup> Meanwhile, the spread of Zika virus<sup>37,38</sup> and outbreaks of yellow fever<sup>39</sup> have become severe public health

concerns, requiring *Aedes* control. Insecticide knockdown speed is paramount to thwart mosquitoes surviving contact and then reproducing. DFDT and MFDT may be alternatives to compounds currently used for indoor residual spraying malaria prevention among other diseases.<sup>16</sup> The environmental impacts of these compounds have not been evaluated, but in this context they should be considered as different compositions of matter, free of the DDT stigma. Furthermore, the various solid forms of these new compositions exhibit different activities for the demise of *Drosophila* as well as *Anopheles* and *Aedes*, demonstrating that manipulation of solid-state structure is a viable strategy for the design of more effective contact insecticides for mitigating insect-borne diseases, with an accompanying benefit of reducing environmental impact.

DFDT was last manufactured in 1945. Allied military investigators, on discovering the pest control techniques of the German armed forces, were derisive. “The German claims as to

the superior insecticidal action of DFDT in comparison to DDT", reads a military intelligence report, "are not clearly supported by their meager and inadequate tests against houseflies."<sup>40</sup> German credibility in the use of chemical insecticides could not have been lower given the revelations coming from Eastern Europe. The results herein show that DFDT claims were credible and that fluorine substitution for *para*-chlorine atoms in DDT markedly speeds the action of DFDT and MFDT by comparison. This may be considered in vector control strategies of the near future that can no longer rely solely on pyrethroids. A German "silent spring", *der stumme Frühling*, the consequence of the overuse of DFDT if Germany had won the war in Europe, would have been a different story, but one that cannot be imagined at present in the absence of knowing the environmental consequences of the fluorine-substituted congeners, risks that warrant further investigation.

## ■ EXPERIMENTAL SECTION

**Crystallization of Single Crystals of DFDT-I and -II.** Single crystals of DFDT in various crystalline forms were prepared in 20 mL glass vials by slow evaporation from a variety of solutions, listed in Supporting Information, Table S1. Single crystals of DFDT-I for X-ray analysis were prepared by placing small single crystal seeds of DFDT-I in contact with a supercooled melt of DFDT, then heating the melt at 40 °C on a hot stage for 7 days. DFDT-II single crystals for X-ray analysis were prepared in a 20 mL glass vial by slow evaporation from diethyl ether solutions.

**Crystallization of Single Crystals of (R)-MFDT and (S)-MFDT.** Single crystals of (R)-MFDT for X-ray analysis were prepared by placing small single crystal seeds of (R)-MFDT in contact with a supercooled melt of (R)-MFDT, then heating the melt at 50 °C on a hot stage for 2 days. Single crystals of (S)-MFDT for X-ray analysis were prepared in the same way as single crystals of (R)-MFDT.

**Crystallization of Single Crystals of (RS)-MFDT-I, -II, and -III.** The (RS)-MFDT-I single crystals for X-ray analysis were prepared in a 20 mL glass vial by slow evaporation from dichloromethane solutions. Heterogeneous nucleation of (RS)-MFDT-II and (RS)-MFDT-III crystals were induced by placing single crystals of (R)-MFDT or (S)-MFDT in contact with supercooled melt of (RS)-MFDT at 30–50 °C and room temperature, respectively. The (RS)-MFDT-II single crystals for X-ray analysis were prepared by placing small single crystal seeds of (S)-MFDT in contact with a supercooled melt of (RS)-MFDT, which was then heated at 35 °C for 2 weeks. The (RS)-MFDT-III single crystals for X-ray analysis were prepared by placing small single crystal seeds of (S)-MFDT in contact with a supercooled melt of (RS)-MFDT, which was then allowed to stand at room temperature for 1 day.

**Preparation of the Amorphous State of DFDT, (RS)-MFDT, (R)-MFDT, (S)-MFDT, and DDT.** The amorphous states of insecticides were prepared by fine mist spraying of a variety of solutions, listed in Supporting Information, Table S2.

**Preparation of Samples in Different Solid-State Forms for Lethality Measurements.** Microcrystals of DFDT-I, prepared by grinding DFDT-I crystals, grown from hexane solutions, using a mortar and pestle, were DFDT-I by powder X-ray diffraction (PXRD). Microcrystals of DFDT-II, prepared by grinding the DFDT-II crystals grown from diethyl ether solutions, contained 93% DFDT-II and 7% DFDT-I by PXRD. Microcrystals of (RS)-MFDT-I, prepared by grinding (RS)-MFDT-I crystals grown from dichloromethane solutions, were pure (RS)-MFDT-I by PXRD. Microcrystals of (RS)-MFDT-II, prepared by grinding the (RS)-MFDT-II crystals grown from the melt, contained a small amount of (RS)-MFDT-I (94% (RS)-MFDT-II and 6% (RS)-MFDT-I) by PXRD. Microcrystals of (RS)-MFDT-III, prepared by grinding the (RS)-MFDT-III crystals grown from the melt, contained a small amount of (RS)-MFDT-I (96% (RS)-MFDT-III and 4% (RS)-MFDT-I) by PXRD. Microcrystals of (R)-MFDT, prepared by

grinding (R)-MFDT crystals grown from dichloromethane solutions, were pure (R)-MFDT by PXRD. Microcrystals of (S)-MFDT, prepared by grinding (S)-MFDT crystals grown from dichloromethane solutions, were pure (S)-MFDT by PXRD. Microcrystals of DDT-I, prepared by grinding commercially obtained DDT crystals (Sigma-Aldrich), were pure DDT-I by PXRD. DDT-II was prepared by evaporation, under room conditions, of a 5 wt% DDT-methyl propionate solution on a glass slide, which produced a crystalline DDT film. The film was then scraped from the slide to give microcrystals containing 60% DDT-II and 40% DDT-I, by PXRD. Amorphous forms of DFDT, (RS)-MFDT, (R)-MFDT, (S)-MFDT, and DDT were prepared by fine mist spraying of their respective hexane solutions onto the top and bottom of 10.0 cm polystyrene Petri dishes, followed by evaporation of hexane, resulting in the amorphous insecticides on both surfaces.

**Lethality Measurements for Amorphous and Crystalline Insecticides.** The lethality of solid-state forms of insecticides was determined by the residual exposure method. Each crystalline form was ground to a particle size similar to that of the amorphous particles prepared by fine mist spraying (Supporting Information, Figure S15). Lethality measurements were performed in duplicate for each solid-state form, each accompanied by two controls (no insecticide). Each microcrystalline form was added to a 10 cm diameter polystyrene Petri dish (2.0 mg per dish for fruit flies, 1.0 mg per dish for mosquitos), which was subsequently shaken to disperse the microcrystals throughout the Petri dish. Amorphous forms were prepared by fine mist spraying a stock solution containing 70 or 35 mg of the respective insecticide in 10 mL hexane onto the top and bottom of 10 cm diameter polystyrene Petri dishes (two sprays = 0.280 mL) and allowing the hexane to evaporate at room temperature, resulting in 2.0 or 1.0 mg of amorphous insecticide in each Petri dish. Adults mosquitos (*Anopheles quadrimaculatus* or *Aedes aegypti*) or fruit flies (*Drosophila melanogaster*) were sedated with carbon dioxide and 25 female mosquitos or flies were transferred to each Petri dish. The top of the dish was then placed over the bottom, and the motion of the mosquitos or fruit flies was recorded with a video camera (Sony HDR-CX455). The knockdown time was measured for each individual insect, with knockdown associated with an insect laying on the bottom surface of the Petri dish in a supine position without moving from its original position after 10 s.

**Statistical Analyses.** Logistic regression of knockdown-time curves was performed to obtain the median knockdown time ( $KT_{50}$ ) of the test flies and mosquitos, the 95% confidence intervals (CI), slopes, and standard errors (SE) using Qcal software.<sup>33</sup>

## ■ ASSOCIATED CONTENT

### 📄 Supporting Information

The Supporting Information is available free of charge on the ACS Publications website at DOI: 10.1021/jacs.9b08125.

Raman spectra of solid-state forms; powder X-ray diffraction patterns; growth of (RS)-MFDT-II and -III by seeded nucleation; single crystals with Miller indices; preparation of DFDT and MFDT crystals; elution data for chiral resolution of (RS)-MFDT; crystal structure of (RS)-MFDT-II and selected crystal data for DFDT-I and -II, (RS)-MFDT-I, -II, and -III, (R)-MFDT, and (S)-MFDT; differential scanning calorimetry; polymorphic compositions; timeline of the % transformation of polymorphs; powder X-ray diffraction patterns of DFDT-II microcrystals during transformation to DFDT-I; preparation of amorphous DFDT and MFDT by fine mist spraying; particles of solid-state forms of DFDT, MFDT, and DDT used for lethality measurements; logistic regression of knockdown-time curves for *D. melanogaster* exposed to solid-state forms of DFDT, MFDT, and DDT; parameters obtained from logistic regression of knockdown-time curves for *D.*

*melanogaster*; median knockdown times of lethality of *D. melanogaster*; lethality measurements of vapor of DFDT, (RS)-MFDT, and DDT for *D. melanogaster*; median knockdown times of lethality measurements of amorphous DFDT, (RS)-MFDT, and DDT against *D. melanogaster*, *A. quadrimaculatus*, and *Ae. aegypti*; NMR spectra; and molecular structures depicted as ellipsoids in 50% probability (PDF)

X-ray crystallographic data for DFDT-I and -II, (RS)-MFDT-I, -II and -III, (R)-MFDT, and (S)-MFDT (CIF)

Video S1, lethality measurements of amorphous DFDT, DFDT-I, and DFDT-II microcrystals for *D. melanogaster* (MP4)

Video S2, lethality measurements of amorphous (R)-MFDT, (RS)-MFDT, and (S)-MFDT for *D. melanogaster* (MP4)

Video S3, lethality measurements of (R)-MFDT, (RS)-MFDT-I, and (S)-MFDT microcrystals for *D. melanogaster* (MP4)

Video S4, lethality measurements of (RS)-MFDT-II and -III microcrystals for *D. melanogaster* (MP4)

Video S5, lethality measurements of DDT-I and -II microcrystals for *D. melanogaster* (MP4)

Video S6, lethality measurements of DFDT-I and -II, (RS)-MFDT-I, and DDT-I microcrystals for *A. quadrimaculatus* (MP4)

Video S7, lethality measurements of DFDT-I and -II, (RS)-MFDT-I, and DDT-I microcrystals for *Ae. aegypti* (MP4)

Video S8, lethality measurements of amorphous DFDT, (RS)-MFDT, and DDT for *D. melanogaster* (MP4)

Video S9, lethality measurements of amorphous DFDT, (RS)-MFDT, and DDT for *A. quadrimaculatus* (MP4)

Video S10, lethality measurements of amorphous DFDT, (RS)-MFDT, and DDT for *A. aegypti* (MP4)

## AUTHOR INFORMATION

### Corresponding Authors

\*mdw3@nyu.edu

\*bart.kahr@nyu.edu

### ORCID

Chunhua T. Hu: 0000-0002-8172-2202

Jingxiang Yang: 0000-0002-0859-6668

Leo A. Joyce: 0000-0002-8649-4894

Michael D. Ward: 0000-0002-2090-781X

Bart Kahr: 0000-0002-7005-4464

### Notes

The authors declare no competing financial interest.

## ACKNOWLEDGMENTS

This work was primarily supported by the New York University Materials Research Science and Engineering Center (MRSEC) program of the National Science Foundation under award number DMR-1420073. The NYU X-ray facility is supported partially by the NSF under Award Number CRIF/CHE-0840277.

## REFERENCES

(1) Tu, T. The discovery of artemisinin (qinghaosu) and gifts from Chinese medicine. *Nat. Med.* **2011**, *17*, 1217–1220.

(2) Simon, C. *DDT: Kulturgeschichte einer Chemischen Verbindung*; Christoph Merian Verlag: Basel, 1999.

(3) Kilgore, L. B. New German Insecticides. *Soap Sanit. Chem.* **1945**, *21*, 138–139.

(4) Brooks, G. T. *Chlorinated Insecticides, Vol. I: Technology and Application*; CRC Press: Cleveland, OH, 1974.

(5) Simmons, J. S. How magic is DDT? *Saturday Evening Post* **1945**, *217*, 18–19.

(6) Kinkela, D. *DDT and the American Century: Global Health, Environmental Politics, and the Pesticide That Changed the World*; UNC Press: Chapel Hill, NC, 2011.

(7) Hall, S. A. *Insecticides, Insect Repellents, Rodenticides and Fungicides of I. G. Farbenindustrie, A. G. Elberfeld and Leverkusen*; Combined Intelligence Objectives Sub-Committee: London, 1945.

(8) Nobel Foundation. *Nobel Lectures: Physiology or Medicine 1942–1962*; Elsevier: Amsterdam, 1964.

(9) Metcalf, R. L. Some Insecticidal Properties of Fluorine Analogs of DDT. *J. Econ. Entomol.* **1948**, *41*, 416–421.

(10) Sumerford, W. T. *Chemistry and Toxicity of Some Organofluorine Insecticides. Agricultural Control Chemicals*; American Chemical Society: Washington, DC, 1950; pp 160–174.

(11) World Health Organization. *Global Malaria Control and Elimination - Report of a Technical Review*; WHO: Geneva, 2008.

(12) Heckel, D. G. Insecticide Resistance After Silent Spring. *Science* **2012**, *337*, 1612–1614.

(13) Carson, R. *Silent Spring*; Houghton-Mifflin, Boston, MA, 1962.

(14) Mandavilli, A. Health agency backs use of DDT against malaria. *Nature* **2006**, *443*, 250–251.

(15) World Health Organization. *Indoor Residual Spraying: An Operational Manual for Indoor Residual Spraying (IRS) for Malaria Transmission Control and Elimination*, 2nd ed.; WHO: Geneva, 2015.

(16) World Health Organization. *Guidelines for Malaria Vector Control*; WHO: Geneva, 2019.

(17) Li, H.; Tsu, C.; Blackburn, C.; Li, G.; Hales, P.; Dick, L.; Bogyo, M. Identification of Potent and Selective Non-covalent Inhibitors of the *Plasmodium falciparum* Proteasome. *J. Am. Chem. Soc.* **2014**, *136*, 13562–13565.

(18) Yoo, E.; Stokes, B. H.; de Jong, H.; Vanaerschot, M.; Kumar, T. R. S.; Lawrence, N.; Njoroge, M.; Garcia, A.; Van der Westhuyzen, R.; Momper, J. D.; Ng, C. L.; Fidock, D. A.; Bogyo, M. Defining the Determinants of Specificity of *Plasmodium* Proteasome Inhibitors. *J. Am. Chem. Soc.* **2018**, *140*, 11424–11437.

(19) Zhao, Y.; Chen, Z.; Chen, Y.; Xu, J.; Li, J.; Jiang, X. Synergy of Non-antibiotic Drugs and Pyrimidinethiol on Gold Nanoparticles against Superbugs. *J. Am. Chem. Soc.* **2013**, *135*, 12940–12943.

(20) Tyler, P. C.; Taylor, E. A.; Fröhlich, R. F. G.; Schramm, V. L. Synthesis of 5'-Methylthio Coformycins: Specific Inhibitors for Malarial Adenosine Deaminase. *J. Am. Chem. Soc.* **2007**, *129*, 6872–6879.

(21) Bohle, D. S.; Debrunner, P.; Jordan, P. A.; Madsen, S. K.; Schulz, C. E. Aggregated Heme Detoxification Byproducts in Malarial Trophozoites:  $\beta$ -Hematin and Malaria Pigment have a Single S = 5/2 Iron Environment in the Bulk Phase as Determined by EPR and Magnetic Mössbauer Spectroscopy. *J. Am. Chem. Soc.* **1998**, *120*, 8255–8256.

(22) Solomonov, I.; Osipova, M.; Feldman, Y.; Baehtz, C.; Kjaer, K.; Robinson, I. K.; Webster, G. T.; McNaughton, D.; Wood, B. R.; Weissbuch, I.; Leiserowitz, L. Crystal Nucleation, Growth, and Morphology of the Synthetic Malaria Pigment  $\beta$ -Hematin and the Effect Thereon by Quinoline Additives: The Malaria Pigment as a Target of Various Antimalarial Drugs. *J. Am. Chem. Soc.* **2007**, *129*, 2615–2627.

(23) Olafson, K. N.; Clark, R. J.; Vekilov, P. G.; Palmer, J. C.; Rimer, J. D. Structuring of Organic Solvents at Solid Interfaces and Ramifications for Antimalarial Adsorption on  $\beta$ -Hematin Crystals. *ACS Appl. Mater. Interfaces* **2018**, *10*, 29288–29298.

(24) Fitzroy, S.-M.; Gildenhuis, J.; Olivier, T.; Tshililo, N. O.; Kuter, D.; de Villiers, K. A. The Effects of Quinoline and Non-Quinoline

Inhibitors on the Kinetics of Lipid-Mediated  $\beta$ -Hematin Crystallization. *Langmuir* **2017**, *33*, 7529–7537.

(25) Olafson, K. N.; Nguyen, T. Q.; Rimer, J. D.; Vekilov, P. G. Antimalarials inhibit hematin crystallization by unique drug-surface site interactions. *Proc. Natl. Acad. Sci. U. S. A.* **2017**, *114*, 7531–7536.

(26) Yang, J.; Hu, C. T.; Zhu, X.; Zhu, Q.; Ward, M. D.; Kahr, B. DDT Polymorphism and the Lethality of Crystal Forms. *Angew. Chem., Int. Ed.* **2017**, *56*, 10165–10169.

(27) Hemingway, J.; Ranson, H.; Magill, A.; Kolaczinski, J.; Fornadel, C.; Gimnig, J.; Coetzee, M.; Simard, F.; Roch, D. K.; Hinzoumbe, C. K.; Pickett, J.; Schellenberg, D.; Gething, P.; Hoppé, M.; Hamon, N. Averting a malaria disaster: will insecticide resistance derail malaria control? *Lancet* **2016**, *387*, 1785–1788.

(28) Riemschneider, R. Kurze Mitteilungen über ein neues Kontaktinsektizid der Klasse der Halogenkohlenwasserstoffe (A Short Communication on a New Contact Insecticide of the Halogenated Hydrocarbon Type). *Süddeutsche Apotheker-Zeitung* **1947**, *87*, 62.

(29) World Health Organization. *A Global Brief on Vector-Borne Diseases*; WHO: Geneva, 2014.

(30) Perryman, M. S.; Harris, M. E.; Foster, J. L.; Joshi, A.; Clarkson, G. J.; Fox, D. J. Trichloromethyl ketones: asymmetric transfer hydrogenation and subsequent Jovic-type reactions with amines. *Chem. Commun.* **2013**, *49*, 10022–10024.

(31) Cantillana, T.; Sundstrom, M.; Bergman, A. Synthesis of 2-(4-chlorophenyl)-2-(4-chloro-3-thiophenyl)-1,1-dichloroethene (3-SH-DDE) via Newman–Kwart rearrangement—A precursor for synthesis of radiolabeled and unlabeled alkylsulfonyl-DDEs. *Chemosphere* **2009**, *76*, 805–810.

(32) Lindquist, A. W.; Jones, H. A.; Madden, A. H. DDT Residual-Type Sprays as Affected by Light. *J. Econ. Entomol.* **1946**, *39*, 55–59.

(33) Lozano-Fuentes, S.; Saavedra-Rodriguez, K.; Black, W. C.; Eisen, L. QCal: A Software Application for the Calculation of Dose–Response Curves in Insecticide Resistance Bioassays. *J. Am. Mosq. Control Assoc.* **2012**, *28*, 59–61.

(34) Matsubara, H. On the Effect of Synthetic Synergists upon the Knockdown Speed of Pyrethroids against Larvae of the Common House Mosquito, *Culex Pipiens Pallens* Coquillett. *Agric. Biol. Chem.* **1967**, *31*, 1130–1134.

(35) Yang, J.; Zhu, X.; Hu, C. T.; Qiu, M.; Zhu, Q.; Ward, M. D.; Kahr, B. Inverse Correlation between Lethality and Thermodynamic Stability of Contact Insecticide Polymorphs. *Cryst. Growth Des.* **2019**, *19*, 1839–1844.

(36) Smol, J. P. Climate Change: A Planet in Flux. *Nature* **2012**, *483*, S12–S15.

(37) Grubaugh, N. D.; Ladner, J. T.; Kraemer, M. U. G.; Dudas, G.; Tan, A. L.; Gangavarapu, K.; Wiley, M. R.; White, S.; Thézé, J.; Magnani, D. M.; Prieto, K.; Reyes, D.; Bingham, A. M.; Paul, L. M.; Robles-Sikisaka, R.; Oliveira, G.; Pronty, D.; Barcellona, C. M.; Metsky, H. C.; Baniecki, M. L.; Barnes, K. G.; Chak, B.; Freije, C. A.; Gladden-Young, A.; Gnirke, A.; Luo, C.; MaInnis, B.; Matranga, C. B.; Part, D. J.; Schaffner, S. F.; Tomkins-Tinch, C.; West, K. L.; Winnicki, D. I.; Cone, M. R.; Kopp, E. W., IV; Hogan, K. N.; Cannons, A. C.; Jean, R.; Monaghan, A. J.; Garry, R. F.; Loman, N. J.; Faria, N. R.; Porcelli, M. C.; Vasquez, C.; Nagle, E. R.; Cummings, D. A. T.; Stanek, D.; Rambaut, A.; Sanchez-Lockhart, M.; Sabeti, P. C.; Gillis, L. D.; Michael, S. F.; Bedford, T.; Pybus, O. G.; Isern, S.; Palacios, G.; Andersen, K. G.; et al. Genomic epidemiology reveals multiple introductions of Zika virus into the United States. *Nature* **2017**, *546*, 401–405.

(38) Metsky, H. C.; Matranga, C. B.; Wohl, S.; Schaffner, S. F.; Freije, C. A.; Winnicki, S. M.; West, K.; Qu, J.; Baniecki, M. L.; Gladden-Young, A.; Lin, A. E.; Tomkins-Tinch, C. H.; Ye, S. H.; Park, D. J.; Luo, C. Y.; Barnes, K. G.; Shah, R. R.; Chak, B.; Barbosa-Lima, G.; Delatorre, E.; Vieira, Y. R.; Paul, L. M.; Tan, A. L.; Barcellona, C. M.; Porcelli, M. C.; Vasquez, C.; Cannons, A. C.; Cone, M. R.; Hogan, K. N.; Kopp, E. W.; Anzinger, J. J.; Garcia, K. F.; Parham, L. A.; Ramirez, R. M. G.; Montoya, M. C. M.; Rojas, D. P.; Brown, C. M.; Hennigan, S.; Sabina, B.; Scotland, S.; Gangavarapu, K.

Grubaugh, N. D.; Oliveira, G.; Robles-Sikisaka, R.; Rambaut, A.; Gehrke, L.; Smole, S.; Halloran, M. E.; Villar, L.; Mattar, S.; Lorenzana, I.; Cerbino-Neto, J.; Valim, C.; Degraeve, W.; Bozza, P. T.; Gnirke, A.; Andersen, K. G.; Isern, S.; Michael, S. F.; Bozza, F. A.; Souza, T. M. L.; Bosch, I.; Yozwiak, N. L.; MaInnis, B. L.; Sabeti, P. C. Zika virus evolution and spread in the Americas. *Nature* **2017**, *546*, 411–415.

(39) Barrett, A. D. T. The reemergence of yellow fever. *Science* **2018**, *361*, 847–848.

(40) Curtis, F. J.; Davis, F. C.; Smadel, J. E.; Southworth, H.; Volwiler, E. H. *Pharmaceuticals and Insecticides at I.G. Farben Plants Elberfeld and Leverkusen*; Combined Intelligence Objectives Subcommittee: London, 1945.